

Effect of the Versatile Bifunctional Chelator AAZTA5 on the Radiometal Labelling properties and the *in vitro* performance of a Gastrin Releasing Peptide Receptor Antagonist

Michael Hofstetter

Department of Nuclear Medicine, Inselspital, Bern, University Hospital

Euy Sung Moon

Department of Chemistry-TRIGA site, Johannes Gutenberg University Mainz

Fabio D'Angelo

Department of Nuclear Medicine, Inselspital, Bern, University Hospital

Lucien Geissbühler

Department of Nuclear Medicine, Inselspital, Bern, University Hospital

Ian Alberts

Department of Nuclear Medicine, Inselspital, University Hospital

Ali Afshar-Oromieh

Department of Nuclear Medicine, Inselspital, Bern, University Hospital

Frank Rösch

Department of Chemistry-TRIGA site, Johannes Gutenberg-University Mainz

Axel Rominger

Department of Nuclear Medicine, Inselspital, Bern, University Hospital

Eleni Gourni (✉ eleni.gourni@insel.ch)

Bern University Hospital <https://orcid.org/0000-0003-2198-382X>

Research article

Keywords: Gastrin Releasing Peptide receptor (GRPr), AAZTA, prostate cancer, imaging, peptide radionuclide therapy

Posted Date: December 3rd, 2020

DOI: <https://doi.org/10.21203/rs.3.rs-57438/v2>

License:  This work is licensed under a Creative Commons Attribution 4.0 International License.
[Read Full License](#)

Version of Record: A version of this preprint was published at EJNMMI Radiopharmacy and Chemistry on November 30th, 2020. See the published version at <https://doi.org/10.1186/s41181-020-00115-8>.

Abstract

Background: Gastrin Releasing Peptide receptor (GRPr)-based radioligands have shown great promise for diagnostic imaging of GRPr-positive cancers, such as prostate and breast.

The present study aims at developing and evaluating a versatile GRPr-based probe for both PET/SPECT imaging as well as intraoperative and therapeutic applications. The influence of the versatile chelator AAZTA⁵ on the radiometal labelling properties and the *in vitro* performance of the generated radiotracers were thoroughly investigated.

The GRPr-based antagonist D-Phe-Gln-Trp-Ala-Val-Gly-His-Sta-Leu-NH₂ was functionalized with the chelator 6-[Bis(carboxymethyl)amino]-1,4-bis(carboxymethyl)-6-methyl-1,4-diazepane (AAZTA⁵) through the spacer 4-amino-1-carboxymethyl-piperidine (Pip) to obtain AAZTA⁵-Pip-D-Phe-Gln-Trp-Ala-Val-Gly-His-Sta-Leu-NH₂ (LF1). LF1 was radiolabelled with gallium-68 (PET), indium-111 (SPECT, intraoperative applications) and lutetium-177 (therapy, SPECT). *In vitro* evaluation included stability studies, determination of lipophilicity, protein-binding studies, determination of K_d and B_{max} as well as internalization studies using the epithelial human prostate cancer cell line PC3. *In vitro* monotherapy as well as combination therapy studies were further performed to assess its applicability as a theranostic compound.

Results: LF1 was labelled with gallium-68, indium-111 and lutetium-177 within 5 min at room temperature (RT). The apparent molar activities (A_m) were ranging between 50-60 GBq/μmol for the ⁶⁸Ga-labelled LF1, 10-20 GBq/μmol for the ¹¹¹In- and ¹⁷⁷Lu-labelled LF1. The radiotracers were stable for a period of 4 h post labeling exhibiting a hydrophilic profile with an average of a LogD_{octanol/PBS} of -3, while the bound activity to the human serum protein was approximately 10%. ^{68/nat}Ga-LF1, ^{177/nat}Lu-LF1 and ^{111/nat}In-LF1 exhibited high affinity for the PC3 cells, with K_d values of 16.3±2.4 nM, 10.3±2.73 nM and 5.2±1.9 nM, respectively, and the required concentration of the radiotracers to saturate the receptors (B_{max}) was between 0.5 and 0.8 nM which corresponds to approximately 4 x 10⁵ receptors per cell. Low specific internalization rate was found in cell culture, while the total specific cell surface bound uptake always exceeded the internalized activity. *In vitro* therapy studies showed that inhibition of PC3 cells growth is somewhat more efficient when combination of ¹⁷⁷Lu-labelled LF1 with rapamycin is applied compared to ¹⁷⁷Lu-labelled LF1 alone.

Conclusion: Encouraged by these promising *in vitro* data, preclinical evaluation of the LF1 precursor are planned in tumour models *in vivo*.

Background

The need to diagnose, prevent, and treat cancer is greater than ever, since cancer-associated deaths are still a major cause of deaths. Early detection is essential for effective treatment of the disease, hence,

many efforts have been made to identify cancer related targets and to further investigate their implication in cancer management (Kumar et al. 2006). The G protein-coupled receptors (GPCR) are of high importance since they have been identified as valuable targets for the development of specific radiotracers for solid tumor imaging in the field of nuclear medicine. The fundamental component for the successful development of GPCR-based radioligands for *in vivo* tumor imaging is the GPCR overexpression on tumors in combination with their low expression and limited density in the surrounding healthy organs (Reubi 2003), with somatostatin receptor being the first to be defined for *in vivo* imaging (Gibril et al. 1996). The successful clinical translation of somatostatin receptor targeting was the driving force for the identification of additional GPCR with the potential to be used for peptide receptor targeted diagnostic and therapeutic applications (Reubi 2013). Gastrin Releasing Peptide receptor (GRPr) that is overexpressed on a variety on human tumors, represents another target with high interest in nuclear medicine (Yu et al. 2013).

A high number of GRPr-based radiotracers, both agonists and antagonists, mainly derived from the N-terminal truncated octapeptide bombesin (7-14), have shown promising results (Mansi et al. 2016). GRPr-based radioagonists were the first to be developed. Although extensive preclinical research has been reported, only few radiotracers have been clinically assessed, mainly because of their mitogenic properties and the side effects. The diagnostic accuracy of the ⁶⁸Ga-labelled BZH3 was investigated in patients with gastrointestinal stromal tumors and gliomas (Dimitrakopoulou-Strauss et al. 2007; Strauss et al. 2012). Clinical trials have also been performed with the GRPr agonist AMBA, labelled with gallium-68 and lutetium-177 in patients with various cancers, to assess its applicability as diagnostic as well as therapeutic radiopharmaceutical (Baum et al. 2007; Bodei et al. 2007). Furthermore, the feasibility of RP527 labelled with technetium-99m was evaluated in patients with prostate and breast cancer (Van de Wiele et al. 2001).

The significant finding of the somatostatin radioantagonists being preferable to radioagonists for *in vivo* peptide receptor targeting (Ginj et al. 2006) stimulated the shift towards the development of GRPr antagonists too (Cescato et al. 2008). A plethora of radioantagonists have been evaluated preclinically and since 2013 several clinical trials have been performed using GRPr radioantagonists (RM2 (or BAY 86-7548), RM26, NODAGA-MJ9, SB3, NeoBOMB1, TE2AAR06, BAY 86-4367) labelled with gallium-68, fluorine-18, copper-64, lutetium-177, with RM2 radiolabelled with gallium-68 being the most deliberated one (Kähkönen et al. 2013; Roivainen et al. 2013; Wieser et al. 2014; Sah et al. 2015; Maina et al. 2016; Nock et al. 2017; Gnesin et al. 2018; Minamimoto et al. 2018; Zhang et al. 2018; Fassbender et al. 2019; Touijer et al. 2019). Baratto et al. recently used RM2 radiolabelled with gallium-68 to map its physiological distribution in humans. Pancreas was the organ with the highest uptake, followed by mild to moderate uptake in the gastrointestinal tract while the radiotracer is eliminated through the urinary tract (Baratto et al. 2019). The above radioantagonists were evaluated in patients with newly diagnosed prostate cancer (PC) and at biochemical recurrence of prostate cancer (BCR PC). In summary, the studies outline that the radioantagonists can be safely administrated to patients. They showed high detection rate of primary PC and BCR PC, were able to detect more lesions compared to [18F]fluoroethylcholine and

[99mTc]Tc-MDP, apparent performance was improved when compared with the radioagonist ⁶⁸Ga-BBN and exhibited higher detection rates compared to MRI. RM2, RM26 and SB3 labelled with gallium-68 have also been used in few pilot studies to evaluate their detection rate in patients with primary breast cancer (Maina et al. 2016; Stoykow et al. 2016; Zang et al. 2018). These studies suggest that GRPr expression is correlated with estrogen receptors (ER) positive tumors, paving thus the way to expand additional the use of GRPr antagonists as a therapeutic tool.

Peptide receptor radionuclide therapy (PRRT) consists an important treatment option especially in the management of inoperable and metastatic tumors (Kwekkeboom et al. 2008). However, several approaches, such as changes of the radioligand, dosimetry and combination therapy with different agents such as radiosensitisers, have been investigated aiming at improving the response rate and survival. Radiosensitization is considered an outstanding addition in cancer treatment. Inhibition of the phosphoinositide 3-kinase protein kinase/mammalian target of rapamycin (PI3K/Akt/mTOR) pathway, which could be activated by PRRT, causes radiosensitization (Gomez-Pinillos and Ferrari 2012). PI3K/Akt/mTOR regulates several physiological functions such as control of cell metabolism, growth, proliferation and survival. Studies also report that PI3K/Akt/mTOR is activated, in particular in 30%–50% of PC, mainly due to the amplification of gene encoding components, advocating that targeted inhibition of those individual components of the signaling cascade might be a solid strategy for cancer therapy (Gomez-Pinillos and Ferrari 2012). Rapamycin which is a mTOR inhibitor, inhibits tumor growth, angiogenesis, metastasis and causes apoptosis in cancer cell lines as well as in tumor mouse models (Konings et al. 2009). The so far attempts to improve the treatment effect of prostate cancer, when using GRPr-analogues, involve dosimetry studies. The first in human dosimetry study with ¹⁷⁷Lu-labelled RM2 was recently published. The therapy was well tolerated without side effects. Pancreas was the dose-limiting organ, bone metastases had the highest uptake, followed by lymph nodes and soft tissue lesions (Kurth et al. 2019). These encouraging data pave the way for more intensive efforts, preclinically as well as in clinical settings, investigating several treatment options of PC.

Herein, the antagonistic statine-based GRPr peptide H-D-Phe-Gln-Trp-Ala-Val-Gly-His-Sta-Leu-NH₂ was functionalized with the chelator 6-[Bis(carboxymethyl)amino]-1,4-bis(carboxymethyl)-6-methyl-1,4-diazepane (AAZTA⁵) via the positively charged spacer 4-amino-1-carboxymethyl-piperidine (Pip) to obtain AAZTA⁵-Pip-D-Phe-Gln-Trp-Ala-Val-Gly-His-Sta-Leu-NH₂ (LF1) (Figure 1). LF1 was radiolabelled with gallium-68, indium-111 and lutetium-177. One of our goals was to investigate the influence of the versatile bifunctional chelator AAZTA⁵ on the GRPr-based antagonist with regard to its receptor binding affinity and the *in vitro* performance of the generated radiotracers. Furthermore, the assessment of its potential in serving as theranostic compound for GRPr-positive tumors, in *in vitro* monotherapy as well as combination therapy studies in the presence of rapamycin, is also reported. The potent GRPr based antagonist RM2 was used as the reference compound (Figure 1).

Materials And Methods

Reagents and Instrumentation

All reagents and solvents were of the best grade available and were obtained from Sigma-Aldrich, Merck, Fluka, AlfaAesar, VWR, AcrosOrganics and Fisher Scientific and used without further purification. They were provided with a septum. All culture reagents were from Gibco BRL, Life Technologies (Grand Island, NY). [177Lu]Lu³⁺ and [111In]In³⁺ were obtained from Isotope Technologies Garching GmbH (ITG) (Munich, Germany) and b.e.Imaging GmbH (Baden-Baden, Germany), respectively. The GalliaPharm® Ge-68/Ga-68 generator was available from Eckert & Ziegler (Berlin, Germany).

Deuterated solvents for Nuclear Magnetic Resonance (NMR) spectra were commercially available by Deutero. Thin layer chromatography plates from Merck, silica gel 60 F254 coated aluminium plates, were used for the analysis. Silica gel 60 (core size 0.063 / 0.200 mm) from Macherey-Nagel was used for purification by column chromatography.

The purification of the peptide was performed by semipreparative Reverse-Phase High Performance Liquid Chromatography (RP-HPLC) on a 120-5 C18 Nucleosil column (250 x 21 mm) applying a linear gradient of 15-90% solvent B in 25 min at a flow rate of 12 mL / min (solvent A, 0.1% trifluoroacetic acid (TFA) / water (H₂O); solvent B, 0.1%TFA / Acetonitrile (ACN)).

The quality control of the peptides as well as the radiolabelled compounds was performed by analytical RP-HPLC from Knauer advanced scientific instrument equipped with a Knauer Smartline Manager 5000, a Smartline Pump 1000 and a Smartline UV Detector 2600. The RP-HPLC runs were performed on an analytical 120-5 C18 Nucleosil column (250 x 4.5 mm) applying a linear gradient of 15-90% solvent B in 25 min at a flow rate of 1 mL / min. (solvent A, 0.1% TFA / H₂O; solvent B, 0.1% TFA / ACN). Ultraviolet detection was performed using a Knauer detector at 240 nm. For radioactivity measurement, a Na(Tl) well-type scintillation Gina star was used. The radiotracer solutions were prepared by dilution with 0.9% NaCl.

The human prostate adenocarcinoma cell line PC3 was obtained from CLS Cell Lines Service GmbH, (Eppelheim, Germany). Cell culture media Dulbecco's Modified Eagle Medium (DMEM) with GlutaMax-I Supplement, F-12 Nutrient Mixture with GlutaMax-I Supplement, Dulbecco's Phosphate Buffered Saline (DPBS), Fetal Bovine Serum (FBS), Trypsin-EDTA and antibiotic solution Penicillin-Streptomycin were from Gibco BRL, Life Technologies (Grand Island, NY) and purchased from ThermoFisher (Switzerland).

Electrospray Ionization - Mass Spectrometry (ESI-MS) mass spectra were acquired on a Bruker Daltonics Esquire 3000 plus device.

The ¹H-, ¹³C-NMR measurements were performed on a Bruker Avance III HD 400 (400 MHz) or Avance III 600 (600 MHz). LC / MS spectra were measured on an Agilent Technologies 1220 Infinity LC system coupled to an Agilent Technologies 6130B Single Quadrupole Liquidchromatography - Mass spectrometry (LC / MS) system.

Thin Layer Chromatography (TLC) scans were acquired on an Elysia Raytest TLC scanner using the Gina Star TLC software.

Quantitative γ -counting was performed with a Cobra II Gamma Counter from Packard Instrument (USA).

All experiments were carried out twice in triplicates.

Synthesis of the prochelator AAZTA⁵-(^tBu)₄

The precursor AAZTA⁵-(^tBu)₄ was successfully synthesized over 4-steps following the protocol described by Sinnes et al. (Sinnes et al. 2019b). Briefly, the synthesis steps are described below and shown in Figure 2:

1,4-Dibenzyl-6-methylpentanoate-6-nitroperhydro-1,4-diazepane (1)

2-nitrocyclohexanone (2.00 g; 13.9 mmol) and Amberlyst A21 (1.05 g) were mixed with dry methanol (MeOH) (35 mL). The solution was heated to 60 °C and stirred under reflux for 1 h. *N,N'*-dibenzylethylenediamine (3.36 g; 13.9 mmol) and paraformaldehyde (1.67 g; 55.5 mmol) were added to the solution. The suspension was heated to 80 °C and stirred overnight. After completion of the reaction, the suspension was filtered and the filtrate concentrated under vacuum. After column chromatographic purification (Cyclohexane (CH) / Ethyl Acetate (EA); 9:1; R_f = 0.27) a yellow oil was obtained as product **1** (5.20 g; 11.8 mmol; 85%).

1,4-Di(tert-butylacetate)-6-methylpentanoate-6-amino-di(tert-butylacetate)-perhydro-1,4-diazepine (3)

1 (1.05 g, 2.39 mmol) was added to a solution containing Pd(OH)₂ / C (0.62 g, 10 wt%) and abs. ethanol (EtOH) (20 mL). Acetic acid (411 μ L; 7.18 mmol) was added, the solution was saturated with hydrogen and stirred overnight at room temperature. After completion of the reaction, Pd(OH)₂ / C was filtered over Celite and the filtrate was concentrated under vacuum. Crude product **2**, a white-yellowish solid, was used for further reaction without further purification.

2 (1.05 g; 2.39 mmol) and K₂CO₃ (1.32 g; 9.57 mmol) were dissolved in dry ACN (30 mL). *tert*-butyl bromoacetate (1.41 mL; 9.57 mmol) and potassium iodide (0.80 g) were added and stirred overnight at 40 °C. The solution was concentrated under vacuum and purified by column chromatography (CH / EA, 7:1; R_f = 0.15). Compound **3** was obtained as yellow oil (0.89 g; 1.30 mmol; 54%).

1,4-Di(tert-butylacetate)-6-pentanoicacid-6-(amino-di(tert-butylacetate))-perhydro-1,4-diazepine (4)

3 (293 mg, 0.43 mmol) was dissolved in 1,4-dioxane / H₂O (2:1; 6 mL). 1 M LiOH solution (641 μ L; 0.64 mmol) was added and stirred overnight at RT. After completion of the reaction, the solution was concentrated, the residue concentrated with 1 M NaHCO₃ solution and extracted several times with chloroform. The organic phase was extracted with H₂O, dried with Mg₂SO₄ and concentrated under vacuum. Compound **4** was obtained a yellowish oil (224 mg; 0.33 mmol; 76%).

Synthesis of the Chelator-Peptide Conjugate

The peptide-chelator conjugate was synthesized manually using standard fluorenylmethoxycarbonyl protecting group (Fmoc) chemistry and Rink amide 4-methylbenzhydrylamine resin. The spacer (Pip) and the prochelator (AAZTA⁵-(^tBu)₄) were consecutively coupled to the peptide using 1-[Bis(dimethylamino)methylene]-1H-1,2,3-triazolo[4,5-b]pyridinium 3-oxid hexafluorophosphate (HATU) as an activating agent. The cleavage of the peptide and the simultaneous deprotection of the side chain-protecting groups was performed using TFA / triisopropylsilane (TIPS) / H₂O (95 / 2.5 / 2.5). The crude conjugate was further purified by semipreparative RP-HPLC as described in the “Reagents and Instrumentation” section.

Radiochemistry

⁶⁸Ga-labelled LF1: The ⁶⁸Ga-labelled radiotracer was prepared within 5 min, using the Modular-Lab PharmTracer module by Eckert & Ziegler (Berlin, Germany). The radiolabeling performance of LF1 was assessed at pH 4.0 (0.2 M sodium acetate buffer), at RT using a conjugate amount of 5 - 20 µg (approximately 3 - 12 nmol). Briefly, the Ge-68/Ga-68 generator was eluted with 5 mL HCl 0.1 N and the eluate (~ 400 MBq) was loaded onto a cation exchange column (Strata-XC, Phenomenex). Gallium-68 was eluted with 700 µL of a mixture of 5.5 M NaCl / 0.1 M HCl directly in a vial containing 400 µL of 1.8 M sodium acetate buffer, 2 mL H₂O, 200 µL of EtOH, 5 mg ascorbic acid / 20 µL H₂O and the tested amount of the conjugate, followed by SepPak C-18 purification to remove uncomplexed radiometal.

¹⁷⁷Lu- and ¹¹¹In-labelled LF1 and ¹⁷⁷Lu-labelled RM2: The ¹⁷⁷Lu- and ¹¹¹In-labelled radiotracers were prepared by dissolving 5-10 µg (approximately 3 - 6 nmol) of LF1 in 250 µL ammonium acetate buffer (0.5 M, pH 5.4), followed by incubation with [¹⁷⁷Lu]Lu³⁺ (30 - 100 MBq) or [¹¹¹In]In³⁺ (approximately 35 - 40 MBq) for 10 min at RT and were used without any further purification step.

After the labelling with gallium-68, lutetium-177 or indium-111 and the quality control of the generated radiotracers, one equivalent of either ^{nat}Ga(NO₃)₃ or ^{nat}LuCl₃ x 6H₂O or ^{nat}InCl₃ x 2H₂O were added to the relevant radiolabelling solutions. The final solutions were incubated at RT for 10 min to obtain structurally characterized homogeneous ligands which were used for the saturation binding studies. The homogeneity was determined by HPLC, showing one peak.

Quality control of the radiotracers / Stability

Chemical and radiochemical purity of the tested solutions were determined using an analytical Nucleosil 100-5 C18 column applying the conditions described in the “Reagents and Instrumentation” section.

The presence of free gallium-68 and ⁶⁸Ga-labelled colloid in the ⁶⁸Ga-labelled LF1 preparation was quantified by radio thin layer chromatography (Radio-TLC) using Silica gel 60-plates and two different mobile phase eluents: a) 0.1 M Na-citrate; b) MeOH / 1 M ammonium acetate (1 / 1, v / v). Using the first Radio-TLC eluent, the radiopeptide product and ⁶⁸Ga-labelled colloid remain immobilized at the starting

point, whereas free gallium-68 move with the mobile phase. When the second eluent is used, only the labelled peptide moves with the mobile phase / solvent front.

The stability of the newly prepared radiotracers was tested via RP-HPLC for a period of 4 h post labeling.

Lipophilicity

The lipophilicity ($\text{LogD}_{\text{octanol/PBS}}$, pH 7.4) was estimated by the “shake-flask” method: The labelled conjugates (100 pmol; 1.1 MBq, 1.2 MBq and 0.5 MBq for ^{68}Ga -, ^{177}Lu - and ^{111}In -labelled LF1 respectively) were added to a solution of 1-octanol (500 μL) and of PBS (500 μL , pH 7.4). The mixture was vortexed for 1 h to reach the equilibrium and then centrifuged (3000 rpm) for 10 min. From each phase, an aliquot (50 to 100 μL) was pipetted out and measured in a gamma-counter. Each measurement was repeated five times. Care was taken to avoid cross-contamination between the phases. The partition coefficient was calculated as the average log ratio of the radioactivity in the organic fraction and the PBS fraction.

Protein binding studies in human plasma

^{68}Ga -, ^{177}Lu - and ^{111}In -labelled LF1 (100 pmol; 1.1 MBq, 1.2 MBq and 0.5 MBq, respectively) were incubated with human plasma (0.5 mL) at 37 °C for 30 min and 60 min respectively. When the incubating period was completed, proteins were precipitated with a solution of 1 mL of MeOH / ACN (1:1). Centrifugation (10 min, 9660g) for the separation of proteins was then performed. After careful separation of the two phases, the respective activities were measured in a gamma-counter, followed by determination of the percentage of each radiotracer which does not bind to the plasma proteins.

Cell culture

The human prostate epithelial adenocarcinoma cell line PC3, which is known to overexpress GRPr, was cultured at 37 °C and 5% CO₂ in Dulbecco's Modified Eagle Medium (DMEM) with GlutaMAX-I supplement and F-12 Nutrient Mix with GlutaMAX-I supplement in a ratio of 1:1. The medium was supplemented with 10% fetal bovine serum (FBS), penicillin (100 U / mL) and streptomycin (100 μg / mL).

Saturation Binding Studies

For receptor saturation analysis, PC3 cells were seeded at a density of 0.8 - 1 million cells per well in 6-well plates and incubated overnight with medium (DMEM : F12 (1:1) containing 1% FBS, 100 U/mL penicillin and 100 $\mu\text{g}/\text{mL}$ streptomycin). The next day, the medium was removed, the cells washed and incubated for 1 h at 37 °C with fresh medium. Afterwards, the plates were placed on ice for 30 min followed by incubation with increasing concentrations of either $^{68/\text{nat}}\text{Ga-LF1}$ or $^{177/\text{nat}}\text{Lu-LF1}$ or $^{111/\text{nat}}\text{In-LF1}$ or $^{177/\text{nat}}\text{Lu-RM2}$ (1-100 nM) in phosphate-buffered saline binding buffer pH 7.4. After the addition of the radioligands, the cells were incubated for 120 min at 4 °C. Non-specific binding was determined in the presence of Tyr⁴-Bombesin at a final concentration of 1 μM . Then the cells were washed twice with ice-

cold PBS, followed by solubilization with 1 N NaOH and the cell-associated radioactivity was measured using a gamma-counter. Specific binding was plotted against the total molar concentration of the added radiotracer. The K_d values and the concentration of the radiotracer required to saturate the receptors (B_{max}) were determined by nonlinear regression using GraphPad (Prism 8 Graph Pad Software, San Diego, CA). For all the cell studies the values are normalized for 1×10^6 cells per well and all data are from two independent experiments with triplicates in each experiment.

Internalization Studies

For internalization experiments, PC3 cells were seeded into 6-well plates and treated as described above. Approximately 0.25 pmol of the respective radiopeptides were added to the medium and the cells were incubated (in triplicates) for 0.5, 1, 2, 4 and 6 h at 37 °C, 5% CO₂ for ¹⁷⁷Lu- and ¹¹¹In-labelled LF1 and for 15, 30, 60, 90, 120, 180 and 240 min at 37 °C, 5% CO₂ for ⁶⁸Ga-labelled LF1. To determine nonspecific membrane binding and internalization, excess of Tyr⁴-Bombesin (final concentration 1 μM) was added to selected wells. At each time point, the internalization was stopped by removing the medium and washing the cells twice with ice-cold PBS. To remove the receptor-bound radioligand, an acid wash was carried out twice with a 0.1 M glycine buffer pH 2.8 for 5 min on ice. Finally, cells were solubilized with 1 N NaOH. The radioactivity of the culture medium, the receptor-bound, and the internalized fractions were measured in a γ-counter.

In vitro therapy studies with ¹⁷⁷Lu-labelled LF1 in the presence or without rapamycin

For the *in vitro* therapy studies, PC3 cells were seeded at a density of 50000-100000 cells (depending on the investigating time point: 100000, 75000 and 50000 cells for 24, 48, 72 h respectively) in 12-well plates and incubated overnight with cultivation medium at 37 °C and 5% CO₂. The next day, the medium was removed, the cells washed, and culture medium containing either rapamycin (10 nM, dissolved in dimethyl sulfoxide (DMSO)) or DMSO (control, the final concentration of DMSO in the culture medium was 0.5%) was added. The plates were incubated at 37 °C and 5% CO₂ for a period of 6 h. Afterwards, the medium containing rapamycin or DMSO was removed and fresh medium was added in each well. Furthermore, 1.85 MBq of ¹⁷⁷Lu-labelled LF1 was added to preselected wells. The monotherapy (either with rapamycin or ¹⁷⁷Lu-labelled LF1 alone) and combination therapy study (¹⁷⁷Lu-labelled LF1 in presence of rapamycin) were performed in parallel with untreated cells which served as reference. The viability of the cells was accessed by the trypan blue exclusion assay after incubation at 37 °C and 5% CO₂ for 24, 48 and 72 h. The experiment was performed twice in triplicate.

Statistical Analysis

All data are expressed as the mean of values ± standard deviation (mean ± SD). Prism 8 Software (GraphPad Software) was used to determine statistical significance at the 95% confidence level, with a P value of less than 0.05 being considered significant.

Results

Synthesis of the prochelator AAZTA⁵-(^tBu)₄

The synthesis route of AAZTA⁵-(^tBu)₄ is shown in Figure 2. First, ring opening of 2-nitrocyclohexanone was carried out *in situ*. A diazepane ring was formed by reaction with *N,N'*-dibenzylidiamine via a double nitro-Mannich reaction, **1**. Hydrogenolysis using Pd(OH)₂ / C and H₂ removed the benzyl protecting groups at the endocyclic amines and simultaneously reduced the nitro group to an amine, **2**. The unstable product was directly reacted with *tert*-butyl bromoacetate without further purification to form tetra alkylated compound, **3**. Deprotection of the methyl ester protecting groups were carried out by using 1 M lithium hydroxide solution and 1,4-dioxane / H₂O (ratio 2:1) to receive the bifunctional chelator AAZTA⁵-(^tBu)₄, **4**.

The analytic data of the intermediate products **1** and **3** as well as the prochelator **4** are presented below:

Product **1**:

MS (ESI⁺): m/z (%): 440.3 (M+H⁺); calculated for C₂₅H₃₃N₃O₄: 439.25

¹H-NMR (CDCl₃, 400 MHz, δ [ppm]): 7.29 (m, 10 H); 3.66 (s, 3 H); 3.67 (dd, J = 13.5 Hz, 4 H); 3.25 (dd, J = 14.0 Hz, 4 H); 2.63 (m, 4 H); 2.12 (m, 2 H); 1.59 (m, 2 H); 1.32 (m, 2 H); 0.78 (m, 2 H). ¹³C-NMR (CDCl₃, 100 MHz, δ [ppm]): 173.6 (s); 139.1 (s); 129.1 (s); 128.3 (s); 127.3 (s); 94.8 (s); 64.9 (s); 61.8 (s); 58.9 (s); 51.5 (s); 36.5 (s); 33.6 (s); 24.6 (s); 22.6 (s).

Product **3**:

MS (ESI⁺): m/z (%): 686.5 (M+H⁺); 708.4 (M+Na⁺); calculated for C₃₅H₆₃N₃O₁₀: 685.45

¹H-NMR (CDCl₃, 400 MHz, δ [ppm]): 3.65 (s, 4 H); 3.61 (s, 4 H); 3.22 (s, 3 H); 2.99 (d, J = 14.1 Hz, 2 H); 2.85-2.65 (m, 4 H); 2.63 (d, J = 14.1 Hz, 2 H); 2.31 (t, J = 7.4 Hz, 2 H); 1.62-1.52 (m, 4 H); 1.44 (s, 18 H); 1.43 (s, 18 H); 1.25 (m, 2 H). ¹³C-NMR (CDCl₃, 100 MHz, δ [ppm]): 174.4 (s); 172.9 (s); 170.9 (s); 80.9 (s); 80.4 (s); 65.3 (s); 63.2 (s); 62.6 (s); 59.4 (s); 52.1 (s); 51.6 (s); 37.3 (s); 34.3 (s); 28.3 (s); 28.3 (s); 25.9 (s); 21.8 (s).

Product **4** (AAZTA⁵-(^tBu)₄):

MS (ESI⁺): m/z (%): 672.4 (M+H⁺); 694.5 (M+Na⁺); calculated for C₃₄H₆₁N₃O₁₀: 671.44

¹H-NMR (CDCl₃, 400 MHz, δ [ppm]): 3.60 (s, 4 H); 3.23 (s, 4 H); 3.00-2.97 (d, J = 14.1 Hz, 2 H); 2.88-2.60 (m, 6 H); 2.36-2.32 (t, J = 7.9 Hz, 2 H); 1.64-1.52 (m, 4 H); 1.43 (s, 18 H); 1.42 (s, 18 H); 1.24 (m, 2 H). ¹³C-

NMR (CDCl_3 , 100 MHz, δ [ppm]): 178.9 (s); 172.9 (s); 170.9 (s); 81.0 (s); 80.5 (s); 65.1 (s); 63.1 (s); 59.4 (s); 52.2 (s); 34.2 (s); 29.8 (s); 28.3 (s); 28.2 (s); 25.6 (s); 22.8 (s); 21.9.

Synthesis of the Chelator-Peptide Conjugate

The synthesis yields of the peptide-chelator conjugate ranged from 30 to 40 %. The purity and identity of the peptides was >95% as determined by HPLC and mass spectroscopy. The analytical data are depicted in Table 1.

A reception control (HPLC and mass spectroscopy) of the compound RM2 (GMP grade) was also performed at our department and the analytical data are reported in Table 1.

Table 1. Analytical data of LF1 and RM2.

Compound	Elemental composition	Purity	Calculated mass	MS (ESI)	Rt (min)
LF1	$\text{C}_{80}\text{H}_{116}\text{N}_{18}\text{O}_{22}$	>95%	1682.89 m/z $[\text{M}+\text{H}^+]$	1623.89 m/z	13.8
RM2	$\text{C}_{78}\text{H}_{118}\text{N}_{20}\text{O}_{19}$	>95%	1638.89 m/z $[\text{M}^+]$	1638.89 m/z	12.8

Radiochemistry / Quality control / Stability

^{68}Ga -labelled LF1:

LF1 (3, 6 and 12 nmol) was labelled with gallium-68 in about 90% radiochemical purity as determined by analytical HPLC, using a UV absorption at $\lambda=240$ nm. The formation of one additional radioactive species (about 10%) was also observed. The retention time of the main peak was 12.8 min while the retention time of the second radioactive species was 12.1 min (Figure 1S). TLC excluded the creation of ^{68}Ga -labelled colloids (Figure 1S). The maximum achieved apparent molar activity (A_m) was approximately 60 GBq / μmol .

^{177}Lu - and ^{111}In -labelled LF1: LF1 was labelled with lutetium-177 and indium-111 at RT in 98% radiochemical purity as determined by analytical HPLC, using a UV absorption at $\lambda=240$ nm. Both analytical methods, HPLC and TLC verified the presence of one radioactive species (the corresponding radiolabelled peptide in each case) while the percentage of the free metal was <2%. The retention times of ^{177}Lu - and ^{111}In -labelled LF1 were 12.7 and 14.5 min respectively (Figure 1S). The apparent molar activities (A_m) were ranging between 10 - 20 GBq / μmol for ^{177}Lu -labelled LF1 and approximately 10 GBq / μmol for the ^{111}In -labelled radioligand.

The stability of all the radiotracers over time was determined with RP-HPLC and neither radiolysis or decomposition was observed for a period of 4 h post labeling.

Lipophilicity / Protein binding studies in human plasma

With a LogD_{octanol/PBS} of -3.2 ± 0.04 , -2.9 ± 0.04 and -2.8 ± 0.08 for the ^{68}Ga -, ^{177}Lu - and ^{111}In -labelled LF1, respectively, all the radiotracers show a hydrophilic profile. (Lipophilicity = the logarithm of the partition coefficient D, where D is the ratio of the distribution of a compound in 2 solvents, here octanol and PBS).

To estimate the bioavailability of the three radiotracers in circulation, the extent of human plasma protein binding was determined. Approximately 10% of the incubating gallium-68, lutetium-177 and indium-111 activity was found to be bound to plasma proteins at the tested time points.

Saturation Binding Studies

Saturation binding studies were performed at 4 °C, in order to allow binding of the radioconjugates to the receptor but to avoid endocytosis. All the radiotracers exhibited affinity for the GRPr positive PC3 cells, with K_d values of 16.3 ± 2.4 nM for $^{68/\text{nat}}\text{Ga-LF1}$, 10.2 ± 2.7 nM for $^{177/\text{nat}}\text{Lu-LF1}$ and 5.2 ± 1.9 nM for $^{111/\text{nat}}\text{In-LF1}$ (Figure 3). The B_{max} values were also at the same level for the three radiotracers (0.4 ± 0.02 nM for $^{68/\text{nat}}\text{Ga-LF1}$, 0.8 ± 0.05 nM for $^{177/\text{nat}}\text{Lu-LF1}$ and 0.6 ± 0.06 nM for $^{111/\text{nat}}\text{In-LF1}$) which correspond to approximately 4×10^5 receptors per cell.

The side-by-side comparison with the high affinity GRPr antagonist RM2 revealed that the affinities of the new tested radiotracers were at the same range with $^{177/\text{nat}}\text{Lu-RM2}$ (K_d: 5.4 ± 0.8 nM and B_{max}: 0.8 ± 0.03 nM).

Internalization Studies

^{68}Ga -, ^{177}Lu - and ^{111}In -labelled LF1 were found to be well associated with the PC3 cells within the incubation time frame (Figure 4). Continued exposure of the cells to the radioactive ligands resulted in a gradual increase of the total cell associated uptake from 15 min to 4 h for ^{68}Ga -labelled LF1 and from 30 min to 6 h for ^{177}Lu - and ^{111}In -labelled LF1. ^{111}In -labelled LF1 exhibited the higher total cell associated uptake (38.3 ± 2.5 %) (Figure 2S) followed by ^{177}Lu -labelled LF1 (34.5 ± 2.3 %) at 6 h (P=0.0035) (Figure 2S). ^{68}Ga -labelled LF1 revealed the lowest cell associated uptake (13.1 ± 0.24 %) (Figure 2S). At 6 h, the amount of specifically internalized activity was 9.2 ± 0.5 % for ^{111}In -labelled LF1 and 8.9 ± 0.8 % for ^{177}Lu -labelled LF1 (P=0.0054), while ^{68}Ga -labelled LF1 exhibited 2.8 ± 0.5 % internalized activity at 4 h. Blocking experiments performed with excess of Tyr⁴-BN, showed negligible nonspecific binding on the cell surface, while less than 0.3% of total added radioactivity was found to be internalized (data not shown) demonstrating the high specificity of the GRPr-conjugates towards PC3 cells.

In vitro therapy studies with ^{177}Lu -labelled LF1 in the presence or without rapamycin

An *in vitro* therapy study was performed aiming at evaluating the effect of combination therapy on PC3 cells (Figure 5). The viability of PC3 cells was verified 48 and 72 h after treatment. The chosen dose of rapamycin for the *in vitro* therapy studies was 10 nM, since it has been previously shown that rapamycin at this concentration has the greatest cytostatic effect on PC3 cells (Dumont et al. 2013). The applied dose of ¹⁷⁷Lu-labelled LF1 was 1.85 MBq. Combination therapy was found to be slightly more effective compared to rapamycin or ¹⁷⁷Lu-labelled LF1 alone (cell viability: approx. 40%, 48 and 72 h after the treatment). The treatment only with rapamycin showed a higher impact compared to ¹⁷⁷Lu-labelled LF1 on PC3 cells (cell viability: approx. 50% for rapamycin and 70 % ¹⁷⁷Lu-labelled LF1 72 h).

Discussion

Prostate cancer, a complex and biologically heterogeneous disease, is the most common type of cancer found in men, which often begins without symptoms. It is on a spectrum varying from asymptomatic and slow-growing to a more aggressive and rapidly progressive systemic malignancy (Kelloff et al. 2009). The survival rate could, therefore, be significantly improved when early detection and personalized treatment take place. Photon emission computed tomography (SPECT) and positron emission tomography (PET) have gained a lot of attention in the management of prostate cancer due to their high accuracy rate. The overexpression of peptide receptors on the surface of prostate cancer cells played a pivotal role in this development and consequently generated interest in the investigation of radiolabelled peptide-based probes for radio-theranostic applications. Prostate Specific Membrane Antigen (PSMA) and GRPr are the two receptors, which are overexpressed on the surface of prostate cancer. Many efforts have been made towards the development of PSMA- and GRPr-based imaging agents with a particular focus on the low molecular weight PSMA inhibitors and the GRPr-based antagonists. PSMA theranostics have proven great success in prostate cancer management in the recent years (Eder et al. 2012; Afshar-Oromieh et al. 2017). However, due to low PSMA expression not all patients suffering from prostate cancer can benefit from the advantages of PSMA targeting. Therefore, there is an urgent need for these patients for both characterization, planning, monitoring of the cancerous disease and treatment itself. Furthermore, because of the noticeable heterogeneity of prostate cancer at the time of diagnosis (Schrecengost and Knudsen 2013), and even more during the recurrence (Scher et al. 2013), it might be possible that the combination of imaging probes would provide clinical advantages with respect to the imaging of various types and stages of prostate cancer. GRPr and PSMA expression were compared on primary prostate cancer samples (Schollhammer et al. 2019; Touijer et al. 2019) as well as patients (Baratto et al. 2020) providing evidence that the biodistribution for the two radioligands were distinct. The so far preliminary data shows that the low metastatic risk PC patients could benefit from GRPr targeting while in high-risk patients the PSMA-based radiotracers could serve as a valuable tool (Minamimoto et al. 2016).

Ongoing research efforts are currently directed to the development of both, PSMA- and GRPr-based radiotracers with a particular focus of bridging radiopharmaceuticals within a theranostic framework. The selection of an appropriate chelator, which bears excellent coordination ability for diagnostic and therapeutic radionuclides, consists the key step of this approach. The most frequently used chelator for

radiopharmaceuticals in clinical routine applications, DOTA (1,4,7,10-tetraazacyclododecane-1,4,7,10-tetraacetic acid), has shown great ability for binding a variety of radiometals such as gallium-68, indium-111, yttrium-90, copper-64, lutetium-177. However, its applicability presents some limitations since efficient radiolabeling yields are achieved between 80 and 100 °C and the optimum labeling pH is 3 to 5 (Price and Orvig 2014). NOTA (1,4,7-triazacyclononane-1,4,7-triacetic acid) and its derivative NODAGA (1,4,7-triazacyclononane, 1-glutaric acid-4,7 acetic acid), enable sufficient labeling yields in lower temperatures compared to DOTA but lower specific activities compared to the DOTA-conjugates are reported. The biggest disadvantage of NOTA and NODAGA is that their cavity is not suitable for the incorporation of therapeutic radionuclides such as lutetium-177 (Eisenwiener et al. 2002). The acyclic chelating agent, HBED-CC (*N,N'*-bis-[2-hydroxy-5-(carboxyethyl)benzyl]ethylenediamine-*N,N'*-diacetic acid) which has been used for the functionalization of PSMA-11, allows efficient radiolabelling with gallium-68 even at ambient temperature, but it forms multiple radiolabelled species (Eder et al. 2014). Therefore, a bifunctional chelator which could surmount the above obstacles would be the optimum choice for the development of a new class of radiotracers. AAZTA⁵, a versatile chelator could be considered as a potential candidate for this purpose. While AAZTA was initially developed for the chelation of Gd(III) as an MRI agent (Aime et al. 2004), it was shown that it exhibits high coordination capability for a variety of metal ions such as gallium-68, indium-111, lutetium-177, scandium-44 (Eisenwiener et al. 2002; Waldron et al. 2013; Pfister et al. 2015; Tsionou et al. 2017; Sinnes et al. 2019a). The mesocyclic structure of AAZTA⁵ facilitates efficient labeling with high molar activities with a variety of radionuclides at RT and even at near neutral pH, optimal conditions for small proteins. Throughout this study, our main goal was to investigate whether and how N-terminal modulations, via the coupling with AAZTA⁵, may influence the affinity of the derived GRPr-based radioligand towards GRPr. A particular focus on additional *in vitro* studies would allow us to assess the suitability of these radiotracers for further evaluation. Attention was also given on the radiometal labelling properties of LF1 after its labeling with gallium-68 (PET), lutetium-177 (therapy, SPECT) and indium-111 (SPECT, intraoperative applications).

Radiolabelling of LF1 with lutetium-177 and indium-111 supports its applicability for sufficient labeling under mild conditions, even at nearly neutral pH. The high stability in combination with the hydrophilic character may have resulted in the low binding to the proteins of human serum (around 10%) as shown by our *in vitro* studies.

When LF1 was labelled with gallium-68 two radiolabelled species were observed by radio-HPLC while Waldron et al. reported the presence of three radioactive species when AAZTA was labelled with gallium-68 under the same conditions (Waldron et al. 2013). Since the difference of the retention time between the two observed species was less than 1 min we cannot fully exclude the formation of one additional species. Modification at the iminodiacetate moiety of AAZTA where one of the acetate groups could be replaced by a methyl group may prevent the formation of side products.

The observed differences of ⁶⁸Ga- compared to ¹⁷⁷Lu- and ¹¹¹In-labelled LF1 with regard to their radiochemical purity prompted us to further investigate if their GRPr binding affinity is influenced and to what extent. Additionally, a side-by-side comparison of their binding affinities along with the binding

affinity of $^{177}\text{nat}\text{Lu}$ -RM2, which served as a reference peptide, was also performed. $^{111}\text{nat}\text{In}$ -LF1 (K_d : 5.16 ± 1.94 nM) was the most affine exhibiting a K_d value similar to $^{177}\text{nat}\text{Lu}$ -RM2 (K_d : 5.42 ± 0.84 nM) followed by $^{177}\text{nat}\text{Lu}$ -LF1 (K_d : 10.25 ± 2.73 nM). $^{68}\text{nat}\text{Ga}$ -LF1 (K_d : 16.27 ± 2.45 nM) was still affine towards GRPr, however, the tracer with the lowest affinity almost by a factor of 3 compared to $^{111}\text{nat}\text{In}$ -LF1. Since for AAZTA, the N_2O_4 coordination may also occur in a competitive way with the favorable N_3O_3 coordination, this might be the reason of the decreased affinity of $^{68}\text{nat}\text{Ga}$ -LF1. These findings were further supported by the *in vitro* internalization studies, which demonstrated high and selective binding of ^{68}Ga -, ^{177}Lu - and ^{111}In -labelled LF1 to GRPr overexpressing cells. ^{177}Lu - and ^{111}In -labelled LF1 exhibited a comparable profile in terms of total cell associated uptake and percentage of specific internalized fraction while the corresponding values of ^{68}Ga -labelled LF1 were considerably lower. The surface associated activity exceeded the amount of internalized activity at all-time points for the three tested radiotracers. In previous studies (Mansi et al. 2011), it was shown that RM2 at a concentration of $10 \mu\text{M}$ does not cause any effect on calcium mobilization after its incubation with PC3 cells, while an immunofluorescence assay revealed no receptor internalization of the DOTA-Pip-conjugate RM2. The previously confirmed antagonistic potency of RM2 in combination with our findings led us to the assumption that the introduction of AAZTA⁵ did not change the antagonist features of the statine-based motif and that LF1 retains its GRPr-antagonistic profile.

These data may eliminate the applicability of ^{68}Ga -labelled LF1 as a PET radiotracer. However, AAZTA may be a suitable chelator for other PET radionuclides, such as scandium-44 (Nagy et al. 2017) and copper-64 (Greifenstein et al. 2020) and the potential of LF1 to serve as a PET tracer should be further evaluated. Furthermore, scandium-44 and copper-64 due to their longer half-life (3.97 and 12.7 h, respectively) compared to gallium-68 (67.7 min) allow late imaging. This is of paramount importance especially in case of GRPr expression imaging, since preclinical (Gourni et al. 2014) as well as clinical data (Wieser et al. 2014) have shown that late imaging may be favorable due to the efficient background clearance.

In a next step, the assessment of the potential of LF1 in serving as theranostic compound for GRPr-positive tumors was investigated. An *in vitro* therapy study was executed with the aim to evaluate the effect of combination therapy on PC3 cells (Edlind and Hsieh 2014) after their treatment with rapamycin, a FDA approved specific inhibitor of mTOR. Our preliminary *in vitro* data showed that combination therapy was slightly more effective compared to monotherapy with ^{177}Lu -labelled LF1. These *in vitro* data is only an early evaluation of whether rapamycin before ^{177}Lu -labelled LF1 treatment would have an additive effect; extensive *in vivo* studies needs to be performed to safely suggest if the mTOR kinase inhibition may contribute to the sensitization of the malignant prostate cancer cells to radiation.

In vivo studies are planned to be performed in order verify the preliminary *in vitro* data and further define the ideal therapeutic doses and therapy regimens.

Conclusion

On the basis of the current results, LF1 labelled lutetium-177 and indium-111 appears to have a considerable potential to serve as a versatile probe suitable for SPECT, therapy and intraoperative applications. The ease of LF1 synthesis, the efficient radiolabeling at RT with a variety of radiometals, the stable encapsulation of lutetium-177 and indium-111 by AAZTA⁵ and their favorable *in vitro* performance renders them suitable candidates for further extensive *in vivo* studies.

In vivo studies are planned to be performed which together with the already *in vitro* data may provide a solid evidence for their clinical translation.

Abbreviations

GPCR: G protein-coupled receptors

GRPr: Gastrin Releasing Peptide receptor

PC: prostate cancer

BCR PC: biochemical recurrence of prostate cancer

ER: estrogen receptors

AAZTA⁵: 6-[Bis(carboxymethyl)amino]-1,4-bis(carboxymethyl)-6-methyl-1,4-diazepane

DOTA: 1,4,7,10-tetraazacyclododecane-1,4,7,10-tetraacetic acid

NOTA: 1,4,7-triazacyclononane-1,4,7-triacetic acid

NODAGA: 1,4,7-triazacyclononane, 1-glutaric acid-4,7 acetic acid

HBED-CC: *N,N'*-bis-[2-hydroxy-5-(carboxyethyl)benzyl]ethylenediamine-*N,N'*-diacetic acid

Pip: 4-amino-1-carboxymethyl-piperidine

TFA: Trifluoroacetic acid

TIPS: triisopropylsilane

EtOH: Ethanol

MeOH: Methanol

Fmoc: fluorenylmethoxycarbonyl protecting group

DPBS: Phosphate Buffered Saline

FBS: Fetal Bovine Serum

ESI-MS: electrospray ionization mass spectrometry

NMR: Nuclear Magnetic Resonance

LC-MS: Liquidchromatography–Mass Spectrometry

ESI-MS: Electrospray Ionization - Mass Spectrometry

TLC: Thin Layer Chromatography

RP-HPLC: Reverse-Phase High-performance liquid chromatography

HATU: 1-[Bis(dimethylamino)methylene]-1H-1,2,3-triazolo[4,5-b]pyridinium 3-oxid hexafluorophosphate

HEPES: (4-(2-hydroxyethyl)-1-piperazineethanesulfonic acid)

ACN: Acetonitrile

DMSO: Dimethyl Sulfoxide

MeOH: Methanol

H₂O: Water

A_m: Molar activities

RT: room temperature

MRI: Magnetic resonance imaging

SPECT: Photon emission computed tomography

PET: Positron emission tomography

PSMA: Prostate Specific Membrane Antigen

PI3K: phosphoinositide 3-kinase

AKT: protein kinase B

mTOR: mammalian target of rapamycin

Declarations

Ethics approval and consent to participate

Not applicable.

Consent for publication

All authors gave their consent for publication

Availability of data and materials

All data generated or analyzed during this study are included in this published article.

Competing interests / Funding

All authors declare that they have no competing interest associated with this publication and there has been no significant financial support.

Authors' contributions

All the authors read and approved the final manuscript.

EG, AR and FR have designed the study; MF, ESM, FA, LG performed the chemistry and radiochemistry experiments; MF, FA and LG performed the in vitro experiments; all authors analysed the data. EG and AR wrote and approved the final manuscript.

Acknowledgements

We thank Prof Dr Helmut R. Maecke and Prof. Dr. Philipp T. Meyer from the Department of Nuclear Medicine, University Hospital Freiburg, Germany, for kindly providing us the compound RM2.

References

Afshar-Oromieh A, Holland-Letz T, Giesel FL, Kratochwil C, Mier W, Haufe S, et al. Diagnostic performance of 68Ga-PSMA-11 (HBED-CC) PET/CT in patients with recurrent prostate cancer: evaluation in 1007 patients. Eur J Nucl Med Mol Imaging. 2017 Aug;44(8):1258–68.

Aime S, Calabi L, Cavallotti C, Gianolio E, Giovenzana GB, Losi P, et al. [Gd-AAZTA]-: a new structural entry for an improved generation of MRI contrast agents. Inorg Chem. 2004 Nov 29;43(24):7588–90.

Baratto L, Duan H, Laudicella R, Toriihara A, Hatami N, Ferri V, et al. Physiological 68Ga-RM2 uptake in patients with biochemically recurrent prostate cancer: an atlas of semi-quantitative measurements. Eur J Nucl Med Mol Imaging. 2019 Sep 2;

Baratto L, Duan H, Maecke HR, Iagaru A. Imaging the Distribution of Gastrin Releasing Peptide Receptors in Cancer. J Nucl Med. 2020 Feb 14;

Baum RP, Prasad V, Mutloka N. Molecular imaging of bombesin receptors in various tumors by Ga-68 AMBA PET/CT: First results. *J Nucl Med*. 2007;48:79P.

Bodei L, Ferrari M, Nunn A, Llull J, Cremonesi M, Martano L, et al. Lu-177-AMBA Bombesin Analogue in Hormone Refractory Prostate Cancer Patients: A Phase i Escalation Study with Single-Cycle Administrations. *Eur J Nucl Med Mol Imaging*. 2007;34:S221–S221.

Cescato R, Maina T, Nock B, Nikolopoulou A, Charalambidis D, Piccand V, et al. Bombesin receptor antagonists may be preferable to agonists for tumor targeting. *J Nucl Med*. 2008 Feb;49(2):318–26.

Dimitrakopoulou-Strauss A, Hohenberger P, Haberkorn U, Mäcke HR, Eisenhut M, Strauss LG. 68Ga-labeled bombesin studies in patients with gastrointestinal stromal tumors: comparison with 18F-FDG. *J Nucl Med*. 2007 Aug;48(8):1245–50.

Dumont RA, Tamma M, Braun F, Borkowski S, Reubi JC, Maecke H, et al. Targeted Radiotherapy of Prostate Cancer with a Gastrin-Releasing Peptide Receptor Antagonist Is Effective as Monotherapy and in Combination with Rapamycin. *J Nucl Med*. 2013 May 1;54(5):762–9.

Eder M, Neels O, Müller M, Bauder-Wüst U, Remde Y, Schäfer M, et al. Novel Preclinical and Radiopharmaceutical Aspects of [68Ga]Ga-PSMA-HBED-CC: A New PET Tracer for Imaging of Prostate Cancer. *Pharmaceuticals (Basel)*. 2014 Jun 30;7(7):779–96.

Eder M, Schäfer M, Bauder-Wüst U, Hull W-E, Wängler C, Mier W, et al. 68Ga-complex lipophilicity and the targeting property of a urea-based PSMA inhibitor for PET imaging. *Bioconjug Chem*. 2012 Apr 18;23(4):688–97.

Edlind MP, Hsieh AC. PI3K-AKT-mTOR signaling in prostate cancer progression and androgen deprivation therapy resistance. *Asian J Androl*. 2014;16(3):378–86.

Eisenwiener K-P, Prata MIM, Buschmann I, Zhang H-W, Santos AC, Wenger S, et al. NODAGATOC, a new chelator-coupled somatostatin analogue labeled with [67/68Ga] and [111In] for SPECT, PET, and targeted therapeutic applications of somatostatin receptor (hsst2) expressing tumors. *Bioconjug Chem*. 2002 Jun;13(3):530–41.

Fassbender TF, Schiller F, Mix M, Maecke HR, Kiefer S, Drendel V, et al. Accuracy of [68Ga]Ga-RM2-PET/CT for diagnosis of primary prostate cancer compared to histopathology. *Nucl Med Biol*. 2019;70:32–8.

Gibril F, Reynolds JC, Doppman JL, Chen CC, Venzon DJ, Termanini B, et al. Somatostatin receptor scintigraphy: its sensitivity compared with that of other imaging methods in detecting primary and metastatic gastrinomas. A prospective study. *Ann Intern Med*. 1996 Jul 1;125(1):26–34.

Ginj M, Zhang H, Waser B, Cescato R, Wild D, Wang X, et al. Radiolabeled somatostatin receptor antagonists are preferable to agonists for in vivo peptide receptor targeting of tumors. *Proc Natl Acad Sci USA*. 2006 Oct 31;103(44):16436–41.

Gnesin S, Ciccone F, Mitsakis P, Van der Gucht A, Baechler S, Miralbell R, et al. First in-human radiation dosimetry of the gastrin-releasing peptide (GRP) receptor antagonist ^{68}Ga -NODAGA-MJ9. *EJNMMI Res.* 2018 Dec;8(1):108.

Gomez-Pinillos A, Ferrari AC. mTOR signaling pathway and mTOR inhibitors in cancer therapy. *Hematol Oncol Clin North Am.* 2012 Jun;26(3):483–505, vii.

Gourni E, Mansi R, Jamous M, Waser B, Smerling C, Burian A, et al. N-terminal modifications improve the receptor affinity and pharmacokinetics of radiolabeled peptidic gastrin-releasing peptide receptor antagonists: examples of ^{68}Ga - and ^{64}Cu -labeled peptides for PET imaging. *J Nucl Med.* 2014 Oct;55(10):1719–25.

Greifenstein L, Späth D, Sinnes JP, Grus T, Rösch F. Mild and efficient ^{64}Cu labeling of perhydro-1, 4-diazepine derivatives for potential use with large peptides, proteins and antibodies. *Radiochimica Acta.* 2020 Jul 28;108(7):555–63.

Kähkönen E, Jambor I, Kemppainen J, Lehtio K, Grönroos TJ, Kuisma A, et al. In vivo imaging of prostate cancer using [^{68}Ga]-labeled bombesin analog BAY86-7548. *Clin Cancer Res.* 2013 Oct 1;19(19):5434–43.

Kelloff GJ, Choyke P, Coffey DS. Challenges in Clinical Prostate Cancer: Role of Imaging. *AJR Am J Roentgenol.* 2009 Jun;192(6):1455–70.

Konings IRHM, Verweij J, Wiemer E a. C, Sleijfer S. The applicability of mTOR inhibition in solid tumors. *Curr Cancer Drug Targets.* 2009 May;9(3):439–50.

Kumar S, Mohan A, Guleria R. Biomarkers in cancer screening, research and detection: present and future: a review. *Biomarkers.* 2006 Oct;11(5):385–405.

Kurth J, Krause BJ, Schwarzenböck SM, Bergner C, Hakenberg OW, Heuschkel M. First-in-human dosimetry of gastrin-releasing peptide receptor antagonist [^{177}Lu]Lu-RM2: a radiopharmaceutical for the treatment of metastatic castration-resistant prostate cancer. *Eur J Nucl Med Mol Imaging.* 2019 Sep 3;

Kwekkeboom DJ, de Herder WW, Kam BL, van Eijck CH, van Essen M, Kooij PP, et al. Treatment with the radiolabeled somatostatin analog [^{177}Lu -DOTA 0,Tyr3]octreotate: toxicity, efficacy, and survival. *J Clin Oncol.* 2008 May 1;26(13):2124–30.

Maina T, Bergsma H, Kulkarni HR, Mueller D, Charalambidis D, Krenning EP, et al. Preclinical and first clinical experience with the gastrin-releasing peptide receptor-antagonist [^{68}Ga]SB3 and PET/CT. *Eur J Nucl Med Mol Imaging.* 2016 May;43(5):964–73.

Mansi R, Minamimoto R, Mäcke H, lagaru AH. Bombesin-Targeted PET of Prostate Cancer. *J Nucl Med.* 2016 Oct;57(Suppl 3):67S-72S.

Mansi R, Wang X, Forrer F, Waser B, Cescato R, Graham K, et al. Development of a potent DOTA-conjugated bombesin antagonist for targeting GRPr-positive tumours. *Eur J Nucl Med Mol Imaging*. 2011 Jan;38(1):97–107.

Minamimoto R, Hancock S, Schneider B, Chin FT, Jamali M, Loening A, et al. Pilot Comparison of ⁶⁸Ga-RM2 PET and ⁶⁸Ga-PSMA-11 PET in Patients with Biochemically Recurrent Prostate Cancer. *J Nucl Med*. 2016 Apr;57(4):557–62.

Minamimoto R, Sonni I, Hancock S, Vasanawala S, Loening A, Gambhir SS, et al. Prospective Evaluation of 68Ga-RM2 PET/MRI in Patients with Biochemical Recurrence of Prostate Cancer and Negative Findings on Conventional Imaging. *J Nucl Med*. 2018;59(5):803–8.

Nagy G, Szikra D, Trencsényi G, Fekete A, Garai I, Giani AM, et al. AAZTA: An Ideal Chelating Agent for the Development of ⁴⁴Sc PET Imaging Agents. *Angew Chem Int Ed Engl*. 2017 13;56(8):2118–22.

Nock BA, Kaloudi A, Lymeris E, Giarika A, Kulkarni HR, Klette I, et al. Theranostic Perspectives in Prostate Cancer with the Gastrin-Releasing Peptide Receptor Antagonist NeoBOMB1: Preclinical and First Clinical Results. *J Nucl Med*. 2017 Jan;58(1):75–80.

Pfister J, Summer D, Rangger C, Petrik M, von Guggenberg E, Minazzi P, et al. Influence of a novel, versatile bifunctional chelator on theranostic properties of a minigastrin analogue. *EJNMMI Res [Internet]*. 2015 Dec 15 [cited 2020 Apr 21];5. Available from:
<https://www.ncbi.nlm.nih.gov/pmc/articles/PMC4679714/>

Price EW, Orvig C. Matching chelators to radiometals for radiopharmaceuticals. *Chem Soc Rev*. 2014 Jan 7;43(1):260–90.

Reubi JC. Peptide receptors as molecular targets for cancer diagnosis and therapy. *Endocr Rev*. 2003 Aug;24(4):389–427.

Reubi JC. Old and new peptide receptor targets in cancer: future directions. *Recent Results Cancer Res*. 2013;194:567–76.

Rovainen A, Kähkönen E, Luoto P, Borkowski S, Hofmann B, Jambor I, et al. Plasma pharmacokinetics, whole-body distribution, metabolism, and radiation dosimetry of ⁶⁸Ga bombesin antagonist BAY 86-7548 in healthy men. *J Nucl Med*. 2013 Jun;54(6):867–72.

Sah B-R, Burger IA, Schibli R, Fribe M, Dinkelborg L, Graham K, et al. Dosimetry and first clinical evaluation of the new ¹⁸F-radiolabeled bombesin analogue BAY 864367 in patients with prostate cancer. *J Nucl Med*. 2015 Mar;56(3):372–8.

Scher HI, Morris MJ, Larson S, Heller G. Validation and clinical utility of prostate cancer biomarkers. *Nat Rev Clin Oncol*. 2013 Apr;10(4):225–34.

Schollhammer R, De Clermont Gallerande H, Yacoub M, Quintyn Ranty M-L, Barthe N, Vimont D, et al. Comparison of the radiolabeled PSMA-inhibitor 111In-PSMA-617 and the radiolabeled GRP-R antagonist 111In-RM2 in primary prostate cancer samples. *EJNMMI Res.* 2019 Jun;3(1):52.

Schrecengost R, Knudsen KE. Molecular pathogenesis and progression of prostate cancer. *Semin Oncol.* 2013 Jun;40(3):244–58.

Sinnes J-P, Nagel J, Rösch F. AAZTA5/AAZTA5-TOC: synthesis and radiochemical evaluation with 68Ga, 44Sc and 177Lu. *EJNMMI Radiopharm Chem.* 2019a Aug 1;4(1):18.

Sinnes J-P, Nagel J, Waldron BP, Maina T, Nock BA, Bergmann RK, et al. Instant kit preparation of 68Ga-radiopharmaceuticals via the hybrid chelator DATA: clinical translation of [68Ga]Ga-DATA-TOC. *EJNMMI Res.* 2019b May 23;9(1):48.

Stoykow C, Erbes T, Maecke HR, Bulla S, Bartholomä M, Mayer S, et al. Gastrin-releasing Peptide Receptor Imaging in Breast Cancer Using the Receptor Antagonist (68)Ga-RM2 And PET. *Theranostics.* 2016;6(10):1641–50.

Strauss LG, Koczan D, Seiz M, Tuettnerberg J, Schmieder K, Pan L, et al. Correlation of the Ga-68-bombesin analog Ga-68-BZH3 with receptors expression in gliomas as measured by quantitative dynamic positron emission tomography (dPET) and gene arrays. *Mol Imaging Biol.* 2012 Jun;14(3):376–83.

Touijer KA, Michaud L, Alvarez HAV, Gopalan A, Kossatz S, Gonen M, et al. Prospective Study of the Radiolabeled GRPR Antagonist BAY86-7548 for Positron Emission Tomography/Computed Tomography Imaging of Newly Diagnosed Prostate Cancer. *Eur Urol Oncol.* 2019 Mar;2(2):166–73.

Tsionou MI, Knapp CE, Foley CA, Munteanu CR, Cakebread A, Imberti C, et al. Comparison of macrocyclic and acyclic chelators for gallium-68 radiolabelling. *RSC Adv.* 2017 Oct 24;7(78):49586–99.

Van de Wiele C, Dumont F, Dierckx RA, Peers SH, Thornback JR, Slegers G, et al. Biodistribution and dosimetry of (99m)Tc-RP527, a gastrin-releasing peptide (GRP) agonist for the visualization of GRP receptor-expressing malignancies. *J Nucl Med.* 2001 Nov;42(11):1722–7.

Waldron BP, Parker D, Burchardt C, Yufit DS, Zimny M, Roesch F. Structure and stability of hexadentate complexes of ligands based on AAZTA for efficient PET labelling with gallium-68. *Chem Commun (Camb).* 2013 Jan 21;49(6):579–81.

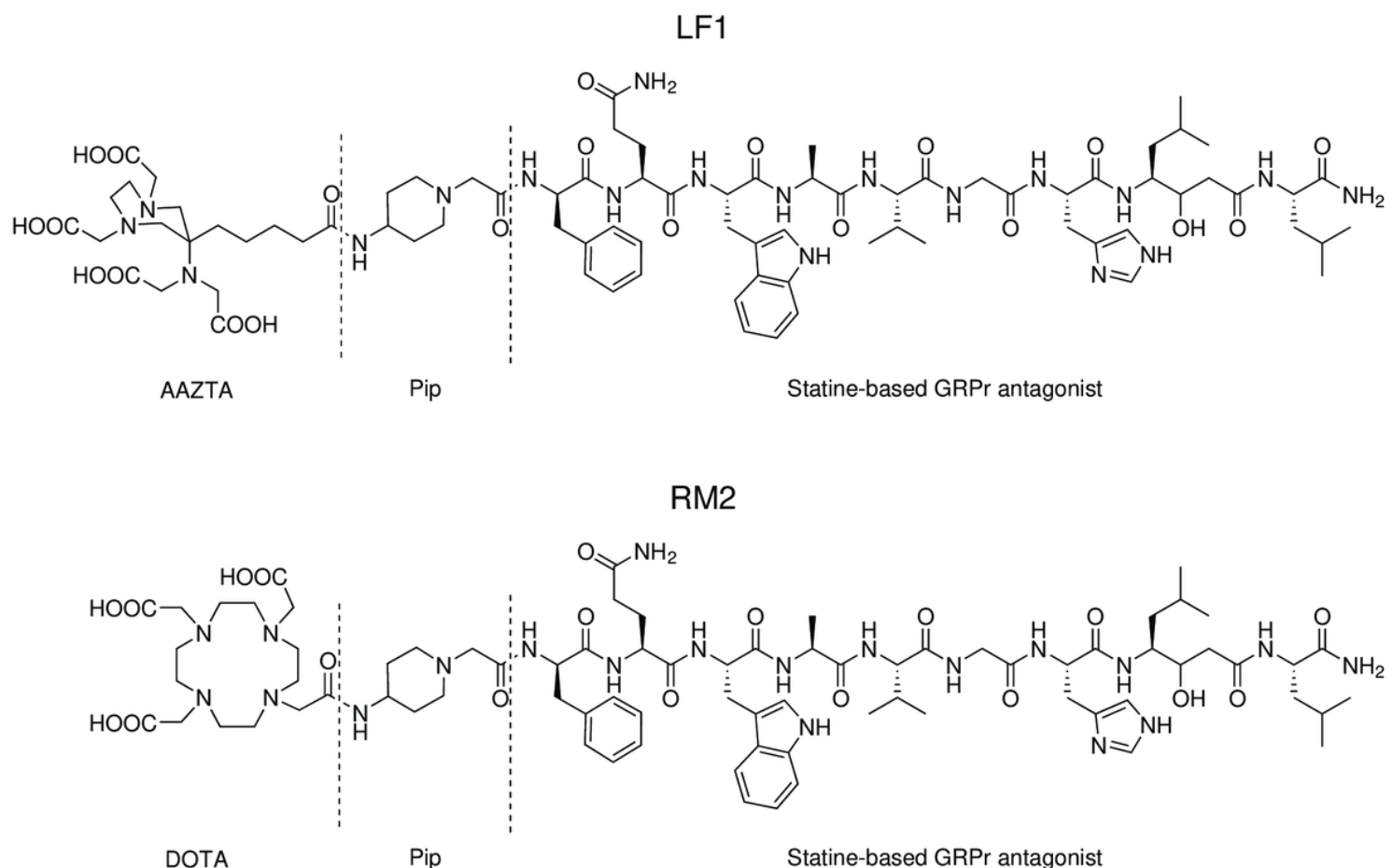
Wieser G, Mansi R, Grosu AL, Schultze-Seemann W, Dumont-Walter RA, Meyer PT, et al. Positron emission tomography (PET) imaging of prostate cancer with a gastrin releasing peptide receptor antagonist—from mice to men. *Theranostics.* 2014;4(4):412–9.

Yu Z, Ananias HJK, Carlucci G, Hoving HD, Helfrich W, Dierckx RAJO, et al. An update of radiolabeled bombesin analogs for gastrin-releasing peptide receptor targeting. *Curr Pharm Des.* 2013;19(18):3329–41.

Zang J, Mao F, Wang H, Zhang J, Liu Q, Peng L, et al. 68Ga-NOTA-RM26 PET/CT in the Evaluation of Breast Cancer: A Pilot Prospective Study. Clin Nucl Med. 2018 Sep;43(9):663–9.

Zhang J, Niu G, Fan X, Lang L, Hou G, Chen L, et al. PET Using a GRPR Antagonist 68Ga-RM26 in Healthy Volunteers and Prostate Cancer Patients. J Nucl Med. 2018;59(6):922–8.

Figures



AAZTA: 6-[Bis(carboxymethyl)amino]-1,4-bis(carboxymethyl)-6-methyl-1,4-diazepane

DOTA: 1,4,7,10-tetraazacyclododecane-1,4,7,10-tetraacetic acid

Pip: 4-amino-1-carboxymethyl-piperidine

Figure 1

Schematic structures of LF1 and RM2.

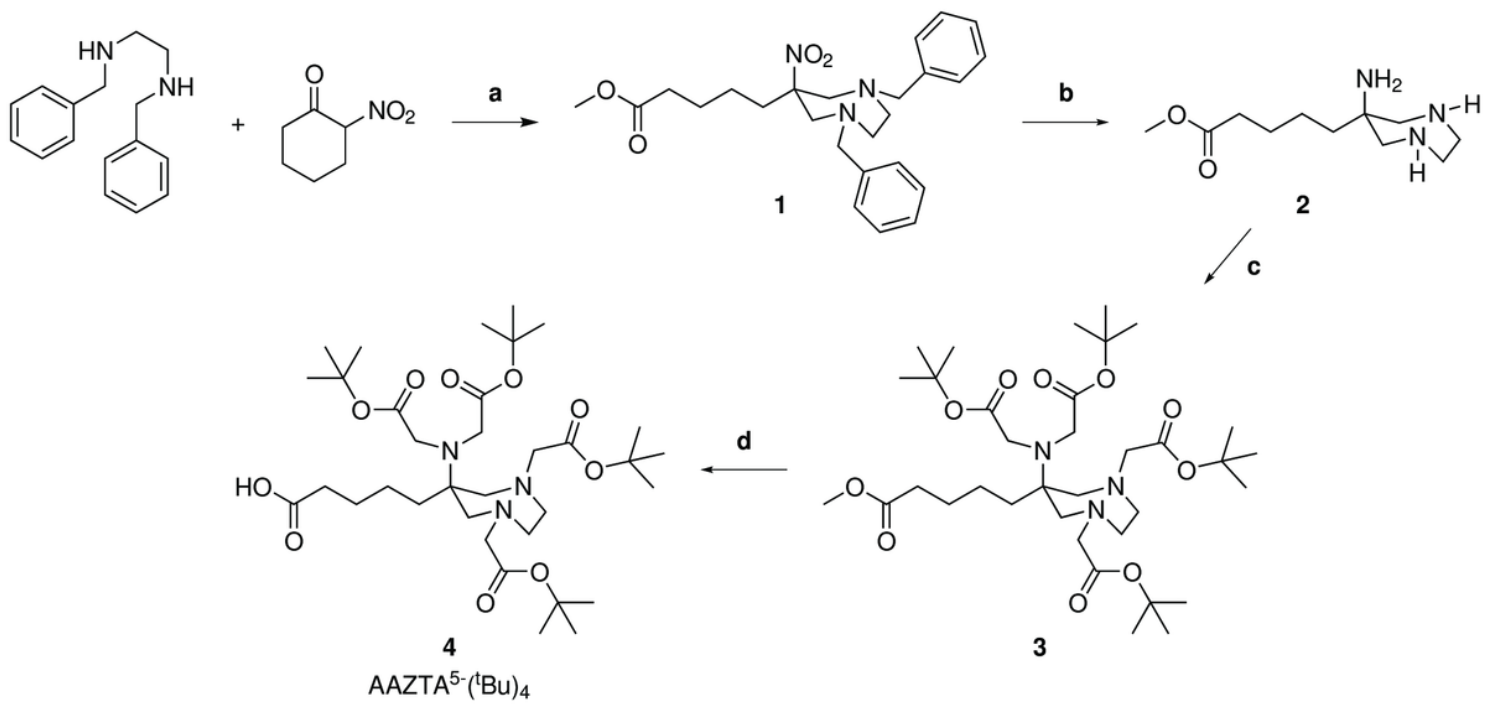


Figure 2

Synthetic scheme of AAZTA5-(tBu)4: (a) paraformaldehyde, MeOH, Amberlyst A21; (b) Pd(OH)₂/C, CH₃COOH, EtOH, K₂CO₃; (c) tert-butylbromacetate, MeCN, K₂CO₃, KI; (d) 1 M LiOH, 1,4-dioxane/H₂O (2:1).

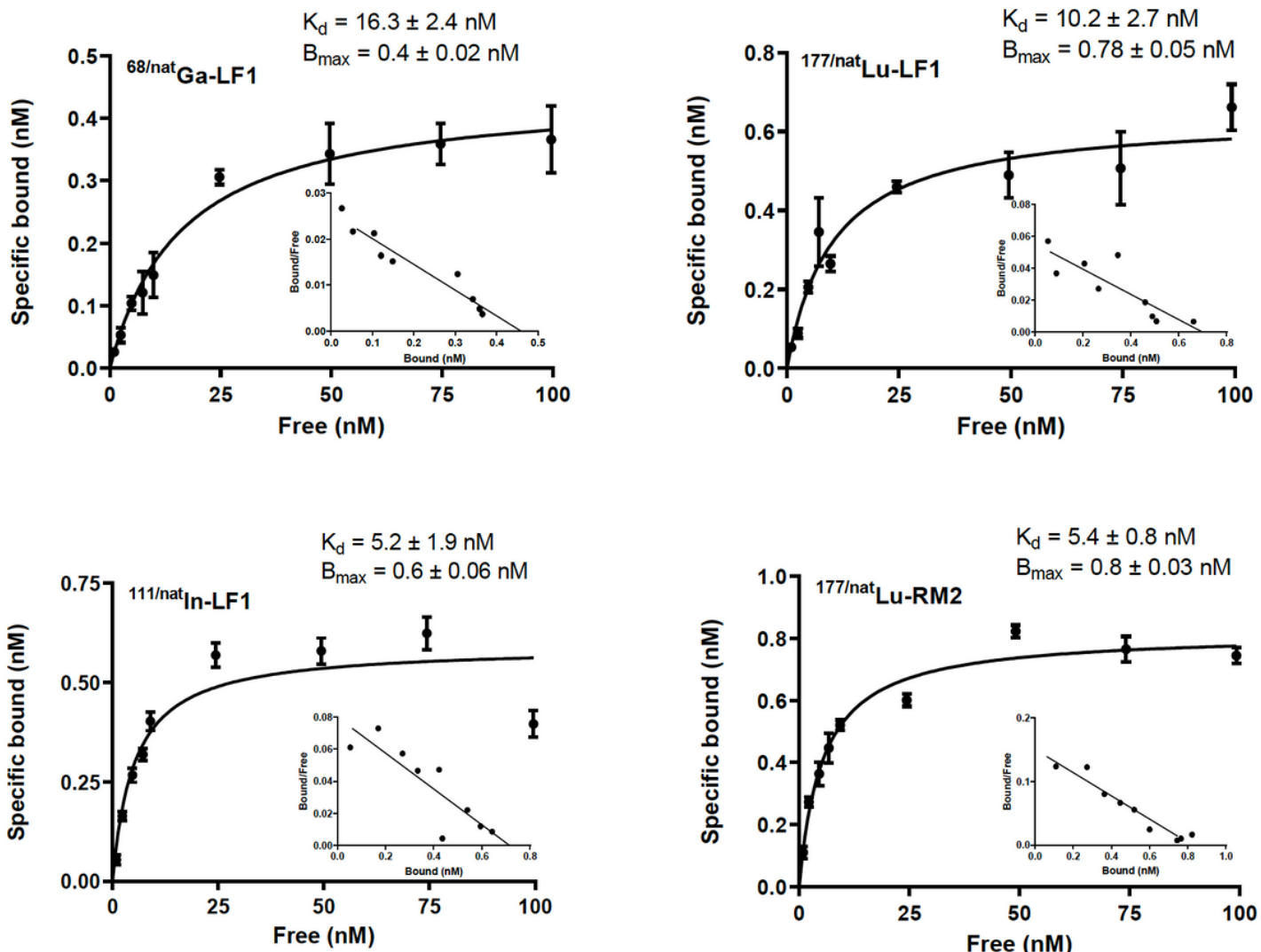


Figure 3

Saturation binding study on intact PC3 cells, using increasing concentrations of ⁶⁸/natGa-LF1, ¹⁷⁷/natLu-LF1, ¹¹¹/natLF-LF1 and ¹⁷⁷/natLu-RM2, ranging from 1 to 100 nM. Dissociation constant (K_d) and maximum number of binding sites (B_{\max}) were calculated from nonlinear regression analysis using GraphPad Prism.

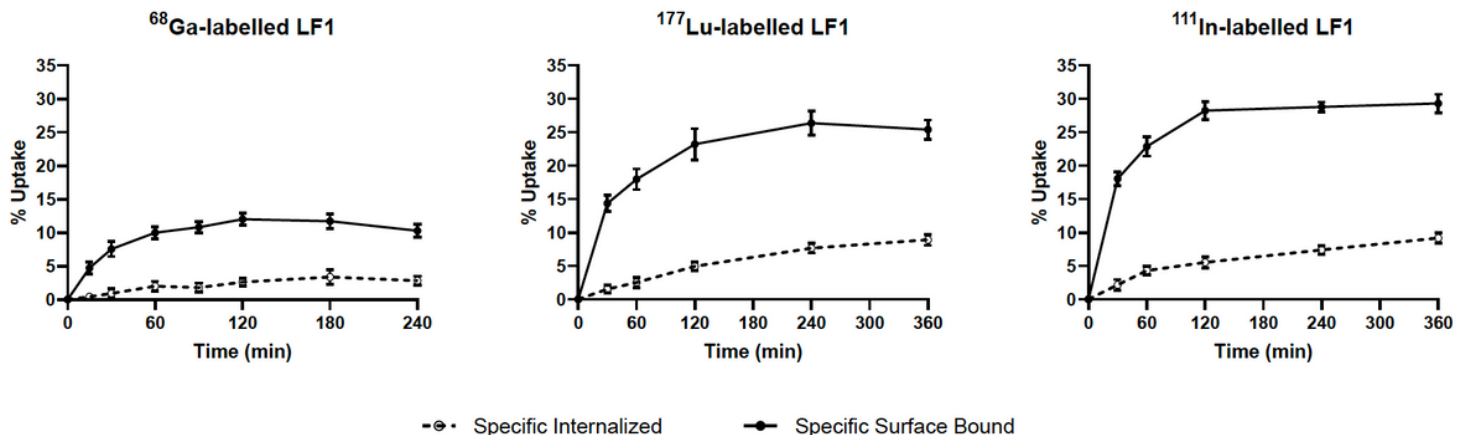


Figure 4

Internalization rate and specific surface bound uptake after the incubation of PC3 cells with 68Ga-, 177Lu-, 111In-labelled LF1 within 4 or 6 h at 37°C. Receptor-specific internalization and specific surface bound activity expressed as percentage of the applied radioactivity. Nonspecific binding was determined in the presence of 1 µM Tyr4-BN.

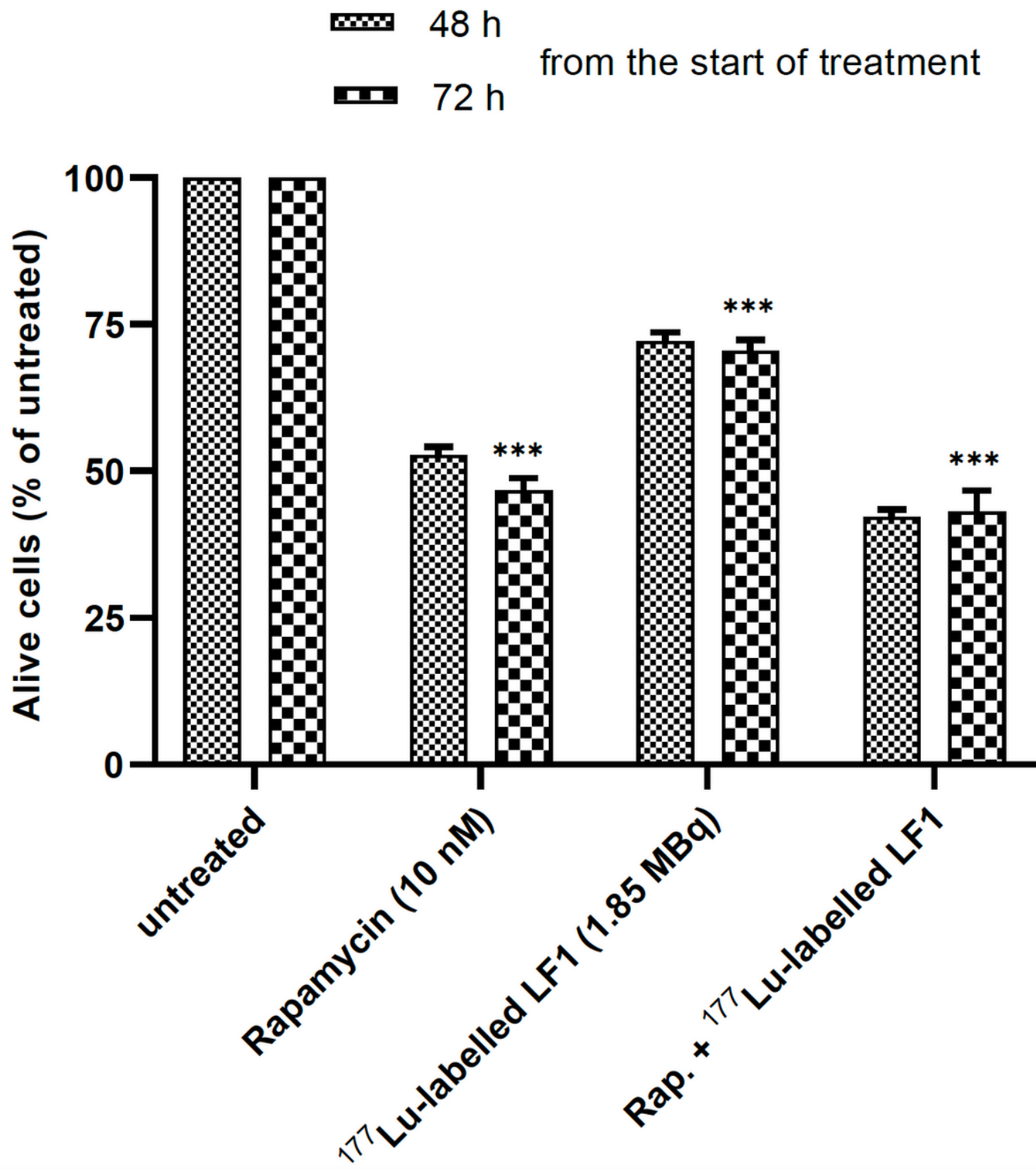


Figure 5

In vitro therapy assessing the effect of monotherapy (rapamycin or 177Lu-labelled LF1) and combination therapy (rapamycin and 177Lu-labelled LF1) on PC3 cells.

Supplementary Files

This is a list of supplementary files associated with this preprint. Click to download.

- [SupplementalDataGourni.doc](#)